FLUVIAL ARCHITECTURE OF THE CERBATANA CONGLOMERATE UNIT (LA VENTA, COLOMBIA) BASED ON DIGITAL OUTCROP MODELS (DOMs) AND HIGH-RESOLUTION STRATIGRAPHY

ELIZABETH ROMERO MONTES[1]

1. Universidad EAFIT, Department of Geology, Medellín, 050022, Colombia

email: eromero2@eafit.edu.co

Abstract

The Miocene sedimentary record in La Venta site in the Neiva Sub-basin of the Upper Magdalena Valley is represented by the Honda Group (La Victoria and Villavieja formations) and corresponds to a sequence of continental origin whose sedimentary record evidence the development of the Central and Eastern Cordilleras of the Colombian Andean System. La Victoria-Villavieja contact is defined by the Cerbatana Conglomerate Unit (CCU) which has been interpreted as a change in the style of sedimentation in response either to a rapid uplift of the paleo-central range or by the input of sediments coming from distal sources. Based on the integration of conventional fieldwork with Digital Outcrop Models (DOMs), in an outcrop that corresponds to the upper part of the CCU six facies were recognized, three are sandstones (Sm, Sft and Sfh) and three are conglomerates (Cmc, Cmm and Cmt). Facies were associated in four stratigraphic architectural components: (1) channels; (2) sand bars; (3) gravel bars; (4) sediment gravity-flow deposits. The studied outcrop described in this study is located in the southeast of La Venta site and it seems to be part of the sedimentary record deposited under a high dynamic braided system.

Key words: La Venta, fluvial architecture, facies analysis, braided river, digital outcrop models.

INTRODUCTION

La Venta site is located in the Neiva Sub-basin (Upper Magdalena Valley) and it is influenced by Quebrada Tatacoa, Quebrada Libano, Quebrada La Venta, and Quebrada Las Lajas (Fields, 1959). Furthermore, it is widely known for being of the major Cenozoic fossil vertebrate localities in South America (Carrillo et al, 2014). Geologically, this location is dominated by a middle Miocene sedimentary record represented by the Honda Group which is divided into La Victoria and Villavieja formations. Units deposited between 13.5 to 12.9 and 12.9 to 11.5 Ma, respectively (Hayashida, 1984; Flynn et al., 1997). Moreover, the contact between these two formations is delimited by an informal sequence called Cerbatana Conglomerate Unit (CCU; Fields, 1959; Wellman, 1970; Guerrero, 1993).

Sedimentological analyses indicated that both La Victoria and Villavieja formations were deposited in meandering fluvial systems caused by the uplift of the Central Cordillera and the Eastern Cordillera (Wellman, 1970; Guerrero, 1993; Villarroel et al., 1996), respectively. On the other hand, CCU accumulation process has been interpreted as the result of a braided river deposition related to a ‘rapid’ paleo-Central range uplifting event (Guerrero, 1993). However, the interpretation of CCU is not fully supported by the data because it has been based on facial analysis of few stratigraphic columns (e.g. Fields, 1959; Wellman, 1970; Guerrero, 1993) which did not include the tremendous lateral extension (~10 km) and the lithological heterogeneity of the body (i.e. sandstones grading to conglomerates at the top toward the west, conglomerates from base to top toward the east, and lateral facies changes from massive clast supported conglomerates with occasional horizontal stratification to conglomeratic sandstones with inclined stratification).

Therefore, the use of only stratigraphic columns offers a limited characterization of the depositional nature of the unit. Here, I hypothesized that the use of digital outcrop models (DOMs) allows the discrimination of architectural fluvial components in the CCU because they give an accurate representation of outcrop faces based on a triangulated irregular network (TIN) that permits to keep real dimensions (Bellian et al., 2005, Burnham & Hodgetts, 2018).

GEOLOGICAL SETTING

The studied CCU outcrop is located in the southeastern part of La Venta site (Figure 1). The stratigraphy of La Venta site records rocks from the Jurassic-Triassic, Miocene and Pleistocene intervals (Fields, 1959; Guerrero, 1993). The middle Miocene sedimentary record is represented by the Honda Group, which is non-conformably overlaying the Jurassic-Triassic record of the Saldaña Formation in angular unconformity, and they are underlain by the rocks of the Neiva and Gigante formations (Villarroel, 1996; Guerrero, 1993). Moreover, the Honda Group sequence is divided in La Victoria and Villavieja formations whose contact between these two formations is delimited by CCU (Fields, 1959; Wellman, 1970; Guerrero, 1993), which is the subject of this paper.

Honda Group

La Victoria formation consists of reddish-brown and greenish-gray mudstones, coarse to fine-grained lithic sandstones (salt and pepper); and coarse-pebble conglomerates (Guerrero, 1993; Villarroel, 1996). In La Venta area, this sequence (462 to 770 meters of thickness) is divided from base to top in the Cerro Gordo Sandstone Beds, Chunchullo Sandstones Beds, Tatacoa Sandstones Beds and Cerbatana Conglomerate Unit (Figure 1). On the other hand, Villavieja Formation (~570 meters of thickness) consists of alternations

of red mudstones facies and medium to fine fine-grained sandstones (Wellman, 1970; Guerrero 1993). This sequence is divided from base to top in the Baraya Member (which includes the units: Monkey Beds, Fish Beds, The Ferruginous Beds and La Venta Red Beds) and the Cerro Colorado member (which includes the units: El Cardon Red Beds, San Francisco Beds and the Polonia Red Beds) (Guerrero, 1993).

Furthermore, both La Victoria and Villavieja formations were deposited as the result of fluvial systems related to the development and uplift of the Central and Eastern Cordilleras of the Colombian Andean System (Wellman, 1970; Guerrero, 1993; Villarroel et al., 1996). Specifically, the lower part of the La Victoria Formation was accumulated under the influence of a meandering fluvial system generated by the gradual uplift of the Central Cordillera (Wellman, 1970; Guerrero, 1993; Villarroel et al., 1996). The upper part of the formation (i.e. CCU) was deposited by a set of braided rivers generated during a (1) 'rapid' uplift of the same mountain range (Guerrero, 1993) or (2) coarser supply from distal segments of the Central Cordillera (Anderson et al. 2016). On the other hand, Villavieja Formation was developed due to the beginning of the Eastern Cordillera which produced a meandering fluvial system (Wellman, 1970; Guerrero, 1993; Villaroel et al., 1996). Moreover, La Victoria and Villavieja formations were deposited from 13.5 Ma to 12.9 Ma and from 12.9 to 11.5 Ma, respectively (Hayashida 1984; Flynn, et al. 1997).

Cerbatana Conglomerate Unit (CCU)

The definition of CCU is still a subject of debate. Fields (1959) called it 'Cerbatana Gravels and Clays'. For him, the unit was composed of massive bedded conglomerates with thickness from around 1 to more than 10 meters, cross bedding sandstones, and siltstones from 10 to 15 centimeters sometimes reaching up to 2 meters thickness. On the other hand,

Guerrero (1993) defined CCU as a clast-supported coarse-pebble conglomerate with lateral extent and thickness of 9 m. Then, Villarroel et al. in 1996, considered the thickness of CCU around 45 meters and lithologically corresponds to matrix-supported conglomerates (clast-supported at some levels) beds with thickness around 10 meters, medium to coarse-grained sandstones and conglomeratic sandstones interlayering the conglomerates which up to 2 m thick, and claystones and siltstones less common in banks from 1 to 11 meters. Besides, CCU definition of Villaroel et al. (1996) seems to be partially equivalent to the unit named 'Rio Seco Conglomerate' (Wellman, 1970) in the northern part of Neiva Sub-basin, which is characterized by ortho-conglomerates beds with a minor component of mudstones layers with an overall thickness of 100 meters.

METHODS

Over the years, surveying techniques have been developed with the purpose to reproduce the three-dimensions features of the outcrops. One of these techniques includes the outcrop digital models (DOMs) are usually scanning from light detection and ranging (LiDAR) and photogrammetry by unmanned aerial vehicles (UAVs) (Charlton et al., 2009; Nesbit et al., 2018). DOMs products are 2D and 3D digital images that can improve the understanding of special facies distribution, as well as the geometry of the rock bodies is not possible to obtain from the classical geological 1D representations (i.e. stratigraphic columns). Furthermore, DOMs are detailed because they are obtained based on triangulated irregular network (TIN) which contains 3D information (X, Y and Z vectors), in contrast with traditional digital elevation models (DEMs) that are generally a raster model in which the Z attribute is extrapolated to the entire pixel, hindering the accurate representation of the faces of an outcrop (Bellian et al., 2005, Burnham & Hodgetts, 2018). Therefore, the

products obtained from DOM offer a visualization of 3D models or 2D orthomosaics (in which all elements are on the same scale unlike traditional or panoramic photographs).

This technique is favorable in the study area due to the high exposure of the rock bodies (tropical dry forest), vertical levels of erosion exposing beds in different outcrop orientation, and the very low deformation of the rock beds (dip angles less than 9°). All these aspects allow to make parallel flights to the shape of the layers.

As mentioned above, there are no studies in Colombia such as the one presented here. Therefore, in order to make the first approach of DOMs for understanding the stratigraphic architecture of an outcrop, I have chosen a site in CCU (Lat: 3.224740, Long: -75.128360) to test the technique and have an insight into the accumulation environment of the unit. The outcrop has a width of 14.8 meters and a thickness of 5.8 meters. This outcrop was chosen given its complexity estimated by the appearance of various beds with sedimentary structures and the lateral and vertical changes of facies on it (Figure 2)

Data collection

A UAV was used to execute the flights. Survey was conducted with an oblique orientation (90° degrees) of the onboard camera to acquire images (orthomosaics) from parallel and convergent views from the outcrop.

Obtaining field data

A stratigraphic column in the southeast of the La Venta site (base, lat: 3.226290, long: -75.125989; top, lat: 3.216692, long: -75.130329) was measured to understand the stratigraphic relationships of CCU with both La Victoria and Villavieja formations. Also, it was necessary to describe, in a detailed fashion (i.e. centimetric descriptions), the

lithological and stratigraphical features of the chosen outcrop: 3 stratigraphic sections measured in the right and left corners and in the center (columns a, b, c in Figure 2a) to add high-resolution geological data to the DOMs. Furthermore, grain size of sediments was defined according to Wentworth (1922), rock color was determined following Munsell's chart (2009), cross-stratification was used to determine paleo-currents directions, and sedimentological and stratigraphic data was plotted using the R package 'SDAR' (Ortíz et al., 2015).

Post-processing

Obtaining a photo-realistic model

Drone-based mapping generates a collection of data points assembled in a digital space (Hodgetts, 2009). According to Bellian et al., (2005), Buckley et al., (2008), and Burnham & Hodgetts (2018) the process to obtain DOMs orthomosaics (3D and 2D) requires to: (1) adjust the dataset to a set of coordinates; (2) assemble the dataset to coaxially mounted RGB images; (3) generate a triangulated mesh and a triangulated irregular network (TIN) based on the dataset and finally; and (4) produce a photo-realistic model by meshing the surface mapped with the image. Agisoft Metashape® software was used to obtain 2D and 3D models (Figure 2, a and c).

Extraction of geological features

Outcrop mapping was made by grouping facies into polygons (Figure 2, a). Then, using the open source software QGIS® it was possible to include the real dimensions of the outcrop. After that, facies assemblages were described and classified in terms of textural and structural properties supported on the integration of field data and digital datasets. Paleocurrents directions were measured using the software OpenplotPj® in the 3D model

(Figure 2, c) and then, both empirical and 3D paleo-current data were analyzed in rose diagrams using the software Stereonet®.

RESULTS

Description of Honda Group

The stratigraphic column (Figure 3) measured in the southeast of the La Venta site, has a thickness of 57.31 meters, showing a sedimentary record belonging to the Honda Group. The stratigraphic thickness of the lower part of La Victoria Formation is 13.5 meters. Then in a gradational contact, CCU is overlaying La Victoria Formation and it has a thickness of 22.1 meters. Finally, Villavieja Formation is overlaid in a gradational contact to the CCU and it has a thickness of 22 meters.

La Victoria Formation.

The first 12.2 meters of this formation are characterized by intercalations of siltstone and massive fine-grained litharenites beds (beds 1-7, Figure 3). Siltstone beds reach up to 3.1 meters of thickness and have light red colors associated with paleosols (Figure 4, a). On the other hand, litharenites beds are well sorted with sub-rounded to rounded grains and have calcareous concretionary upper surfaces. These sandstones bodies reach up to 1.9 meters of thickness and have pale greenish yellow fresh color. The aforementioned sequence is overlaid by a bed (0.7 meters of thickness) dominated by the intercalation of fine-grained and very fine-grained feldespathic litharenites laminas (bed 8, Figure 3). Then, bed 8 is overlaid by a thick layer (0.6 meters of thickness) of moderate greenish yellow siltstone (bed 9, Figure 3).

Cerbatana Conglomerate Unit (CCU).

The upper part of La Victoria Formation, which corresponds to CCU, in general could be defined by beds of sandstones with trough cross-stratification (base of the sequence, Figure

3) and layers of matrix- to clast-supported conglomerates (upper part of the sequence, Figure 3). Specifically, one could describe CCU from base to top as a bedset (13.5 to 28.4 meters) composed by very thick beds (reaching up to 5.5 meters of thickness) of medium to medium-coarse litharenites and feldespathic litharenites with the presence of through cross-stratification (beds 10, 11, 12, 13, 14, 15, Figure 3) and a fine-grained litharenite which corresponds to bed 16 (Figure 3). These sandstones are well to moderated sorted and have sub-rounded to rounded clasts. Some of them (beds 10, 11 and 15, Figure 3) have a granully to pebbly admixture (10-15%) and mud intraclasts which reach 4 cm in diameter. These mud intraclasts follow the cross-stratification in some cases as in bed 10 (Figure 4, b). Besides, sandstones bodies present calcareous concretions within beds and pale greenish yellow (beds 10, 11, 12 and 14) or grayish yellow color (bed 15, Figure 3).

From the 28.4 to 35.6 meters, CCU sequence is composed by trough cross-stratified and massive matrix supported conglomerates (bed 17 and 18, Figure 3), a clast-supported conglomerate that changes in the lateral extension to conglomeratic sandstones with trough cross-stratification (bed 19, Figure 3), and a medium-grained feldespathic litharenite (bed 20, figure 3). These matrix-supported conglomerates have medium to coarse (bed 17, Figure 3) and fine to medium (bed 18, Figure 3) sandy matrix and they present sub-rounded to rounded gravel clasts that reach 6 centimeters in diameter. Matrix percent varies between 25% (bed 17, Figure 3) and 50% (bed 18, Figure 3). In bed 19, clast-supported conglomerate changes in the lateral extension to conglomeratic sandstones with trough cross-stratification (thickness reaches 1.7 meters). This bed presents sub-rounded to rounded gravel clasts that reach 6.5 and 5.5 centimeters in diameter, respectively; and mud intraclasts. Finally, bed 20 corresponds to the last one layer of the CCU sequence (thickness reaches 2.6 meters). This bed presents trough cross-stratification and a granully to pebbly

admixture (10%) with sub-rounded to rounded gravel clasts (figure 4, d). Besides, its base is characterized by calcareous nodules and concretions with spheroidal weathering (Figure 4, e).

Villavieja Formation.

The 22 meters of this formation is characterized by intercalations of siltstones and massive fine-grained feldespathic litharenites (Figure 4, f). Siltstones beds reach up to 8.5 meters of thickness (beds 21, 22 and 24, Figure 3) and have light red and reddish orange colors associated with paleosols (Figure 4, g). On the other hand, feldespathic litharenites are well sorted with sub-rounded to rounded grains, and have calcareous concretions at the top and within the beds (Figure 4, h). These sandstones bodies reach up to 1.7 meters of thickness and have pale greenish yellow fresh color (beds 23 and 25, Figure 3). Discontinues flat laminations of heavy minerals (Figure 4, i) are representative.

Facies Analysis

The studied outcrop represents 5.7 meters of the upper part of the CCU sequence. It includes the rocks recorded between the upper part of bed 14 until the top of bed 18 (Figure 3). Results obtained from the high-resolution stratigraphy determined in the field (3 stratigraphic columns) and the orthomosaic (2D model) analysis, summarized in Table 1 and showed in Figure 5, allowed to determine 6 facies: Facies Cmm – Massive matrix supported conglomerate, Facies Cmt – Trough cross-stratified matrix supported conglomerate, Facies Cmc – Massive clast-supported conglomerate, Facies Sfh – planar horizontally stratified sandstones, Facies Smt – Trough cross-stratified medium-grained sandstone, and Facies Sft – Trough cross-stratified fine-grained sandstone.

Facies Cmm – Massive matrix supported conglomerate.

It consists of very poorly sorted, massive matrix-supported conglomerate. Clasts are sub-rounded to rounded and reach 6 centimeters in diameter. This pebble-conglomerate occurs as a single bed (polygon 6, Figure 5.) with a maximum thickness of 1.3 meters. Cmm presents coarse sandy matrix in a proportion of 50% and secondary calcareous cement.

Facies Cmt – Trough cross-stratified matrix supported conglomerate.

It consists of poorly sorted, trough cross-stratified matrix supported conglomerate. Clasts are sub-rounded to rounded and reach 5.7 centimeters in diameter. Cmt presents medium to coarse sandy matrix in a proportion of 25%. This conglomerate occurs mixed with Cmm facies in polygon 5 (Figure 5), which has a thickness of 1.4 meters.

Facies Cmc – Massive clast-supported conglomerate.

It consists of massive clast supported conglomerate, with clast size reaching 5.6 centimeters in diameter. It is mixed with Cmt and shows imbricated clasts in some cases. It was not possible to define sorting, clasts roundness or the matrix type because the facies was identified and defined from the detailed study based on the 2D model and not from field log.

Facies Sfh – planar horizontally stratified sandstones.

It consists of horizontally stratified fine-grained litharenite. Sediments are well sorted and are sub-rounded to rounded. This sandstone occurs as a single bed (polygon 3, Figure 5.) reaching a maximum thickness of 1.3 meters. Bed geometry is sub-tabular with sharp planar base. Black stripes of heavy mineral are commonly forming discontinuous flat lamination.

Facies Smt – Trough cross-stratified medium-grained sandstone.

It consists of medium-grained trough cross-stratified feldespathic litharenite. Sediments are moderately sorted and are sub-rounded to rounded. This sandstone occurs as a single bed

(polygon 2, Figure 5.) reaching a maximum thickness of 1.6 meters. Bed geometry is sub-tabular with sharp planar base. This sandstone has a granully-pebbly admixture (15%), which reaches 4.2 centimeters in diameter. Sedimentary trough-cross bedding structures have ordered imbricated fabric. Smt is interbedded with facies Cmt in polygon 4 as well.

Facies Sft – Trough cross-stratified fine-grained sandstone.

It consists of fine-grained trough cross-stratified feldespathic litharenite. Sediments are well sorted and are sub-rounded to rounded. This sandstone occurs mixed with Sfh facies in polygon 1 (Figure 5), which has an apparent thickness of 0.9 meters because it is covered by eroded material. Polygon 2 (Figure 5) presents facies Sft in a proportion of approximately 5%.

Paleo-currents analysis

Two planes were measured in the 3D model obtaining the direction of the axes of trough cross-stratification (black surfaces, Figure 6). These measurements were made in polygons 2 and 5 obtaining a direction of 133° and 117°, respectively (Figure 6, a and e). Field observations allowed recognizing one set with two vertical faces at right angles in the polygon 2 obtaining 149° as the axis direction (figure 6, b) and eleven sets with one vertical face exposed of trough cross-stratification showing a tendency towards SW (Figure 6, c) with predominant values between 213° and 239°. In the polygon 1, two sets with one vertical face exposed of trough cross-stratification were identified showing a tendency towards SW with values between 190° and 209° (Figure 6, d).

Data integration from the trough cross-stratification axes measured in the field and from the 3D model show a tendency towards the SE (Figure 6, f). All measurements obtained are shown in Table 2.

DISCUSSION

Facies defined in the studied outcrop are associated into 4 stratigraphic architectural components following the definitions of Miall (1985): channels, sand bars, gravel bars, and sediment gravity-flow deposits. These elements are correlated with the CCU sequence described in the southeast of La Venta area and seem to be related to a high dynamic braided river system at the upper part of the unit.

Facies defined in the studied outcrop were interpreted in function of the transportation processes in relation with the texture and the sedimentary structures identified (Collinson & Thompson, 1984). Four facies are related to tractions-dominated bedload by unidirectional currents (Cmt, Cmc, Sft and Smt), one to turbulent sediment transport (Sfh) and one to gravity flow transport (Cmm). The characterization of the facies and their interpretations are shown in Table 3.

The channel element (CH) identified in the polygon 4 (figure 7) comprises facies Smt and Cmt. This element is characterized by a lenticular external shape and is bounded by a basal sharp erosional concave-up surface. Thickness and width of this component reach 0.98 and 11 meters, respectively; with a width/depth ratio is 11.2. According to Miall (1985), width/depth ratios less than 15 are common in a fixed ribbon-shaped geometry. Therefore, these elements are interpreted as a broad channel fill-complex that could have been generated by lateral channel migration enhanced by little subsidence (Miall, 1985).

Moreover, sand bar (SB) elements in polygons 1, 2, and 3 (Figure 7) and comprise Sft, Smt and/or Sfh facies. Polygons 2 and 3 are characterized by tabular external shape and are bounded by a sharp irregular basal surface. Besides, they reach a thickness between 1.6 (polygon 2, Figure 7) and 1.3 meters (polygon 3, Figure 7). In polygon 1, it was not possible to define this component, given that the real thickness of it is covered by eroded material.

Planar stratification in polygon 3 may indicate the interaction between turbulent sediment transport and the migration of low-amplitude bed forms under an upper flow regime (Paola et al., 1989). Besides, facies SB at Sfh could have formed at higher flow velocities than SBs below (i.e. polygon 1 and 2). Consequently, SB elements record intra-channel deposition due to the migration channel bed loads (Collinson & Thompson, 1984; Miall, 1985, 2006).

The gravel bar element (GB, thickness reaches 1.4 meters) in polygon 5 (Figure 7) and it comprises Cmt and Cmc facies. It is characterized by a tabular external shape and is bounded by a sharp irregular basal surface. Cmt and Cmc facies indicate high depositional energy and, therefore, they might represent the migration of transverse bars (Miall, 1985).

Sediment gravity-flow (SG, thickness reaches 1.3 meters) in polygon 6 (Figure 7) is comprised of pebble supported by a matrix of fine to medium sand (Cmm facies). It is characterized by a tabular external shape and is bounded by a sharp irregular basal surface. The absence of sedimentary structures and the poor sorting suggest that deposition of this element could be related with debris flows (Miall, 1985).

First and second-order contacts were identified in the studied outcrop considering the element hierarchy defined by Allen (1983) and adapted by Miall (1985). These contacts represent the boundaries of individual crossbed sets and the margins that delimit the sets of cross-stratification, respectively. Third order contacts were no defined in the mentioned outcrop because its lateral extension does not allow to establish the relationships and associations between architectural elements. Outcrops with large lateral extension are necessary for the satisfactory definition of the element hierarchy.

CCU sequence presented in this study is defined from the evidence of gradational changes with the uppermost beds of La Victoria Formation and the lower beds of Villavieja Formation (Figure 3). Here, I propose to include in this sequence the medium grained

sandstone with concretionary base (bed 20, Figure 3) that is defined in previous studies (e.g. Guerrero, 1993) as the base of the first bed of the Villavieja Formation known as Monkey bed (Figure 8). Therefore, my CCU definition is partially equivalent to the Villarroel's et al. (1996) CCU definition because it was not possible to identify fine-grained facies within the stratigraphic sequence of the CCU. Guerrero's (1993) CCU characterization may correspond to the bed 19 where it was identified the clast supported conglomerate. However, the thickness and the lateral extension that Guerrero (1993) defined for CCU is not equivalent to the fieldwork observations recorded in this study. Sediments exposed in CCU sequence are interpreted as a record of a braided fluvial system considering the predominance of coarse-grained sediments and the absence of fine-grained facies. However, sedimentological observations indicate changes in the hydrodynamic conditions showing a multi-phase nature in its deposition. Therefore, depositional conditions seem to have progressively changed into a high energy braided river system. Consequently, beds of the studied outcrop here seem to be part of the sedimentary record deposited under a high dynamic fluvial system. From bed 20 (Figure 3), flow energy seems to decrease resulting in the subsequent deposition of fine facies of the Villavieja Formation. Depositional environment would correspond to a sand-dominated braided river sequence towards the base (Figure 9, a) and a gravel-dominated sequence towards the top (Figure 9, b and c).

On the other hand, paleo-current data show a narrow range of directions striking to the southeast. This is consistent with previously data reported in CCU, assuming the main source sediment area is to the west side of the basin (Guerrero, 1993).

Finally, this study reveals that DOMs are useful for discriminating architectural elements into the lateral extension of an outcrop. These elements represent sedimentary bodies that

comprise distinctive facies associations related to depositional sub-environments. Future work should pay special attention to lateral and vertical change of facies from the correlation within outcrops along the ~10 km of extension of CCU, as well as provenance studies, with the aim to enhance the stratigraphic details of depositional environment processes and the source area of sediments that defined the sedimentary record of the CCU.

CONCLUSIONS

(1) Six facies were recognized in the studied outcrop, three are sandstones (Sm, Sft and Sfh) and three are conglomerates (Cmc, Cmm and Cmt). They could be clustered into two assemblages: traction-dominated bedload (i.e. Cmt, Cmc, Sft and Smt) and turbulent and gravity flow transport (i.e. Sfh and Cmm).

(2) From the association of facies, 4 stratigraphic architectural components in the studied outcrop were defined: channels, sand bars, gravel bars, and sediment gravity-flow deposits.

(3) Sedimentological observations in CCU sequence shows a multi-phase nature in the deposition that seem to have gradually changed into a high dynamic braided river system. The characterization of CCU sequence in this study is defined from the observed evidence of gradational changes regarding the finer-grained lithologies of both La Victoria and Villavieja formations which were not taken into account in previous studies.

(4) Stratigraphical analysis based on DOMs and high-resolution field data allows to define architectural fluvial elements. However, outcrops with large lateral extension are necessary for the satisfactory definition of the element hierarchy.

ACKNOWLEDGMENTS

This project was supported by the Paleobiology Laboratory of the Smithsonian Tropical Research Institute. Special gratitude goes to Germán Bayona (who proposed the idea of this study), Mauricio Baquero (photogrammetry execution), Daniel Monterrosa (fieldwork assistance) and Manuel Arias (fieldwork assistance).

REFERENCES

Allen, J., 1983. Studies in fluviatile sedimentation: bars, bar-complexes and sandstone sheets (low-sinuosity braided streams) in the Brownstones (L. Devonian), Welsh Borders. Sediment. Geol., 33: 237-293.

Anderson, V. J., Horton, B.K., Saylor, J.E., Mora, A., Tesón, E., Breecker, D., Ketcham, R. (2016). Andean topographic growth and basement uplift in southern Colombia. Implications for the evolution of the Magdalena, Orinoco and Amazon river systems. Geosphere. 12, 1235-1256.

Bellian, J., Kerans, C., Jennette, D. C. (2005). Digital Outcrop Models: Applications of Terrestrial Scanning Lidar Technology in Stratigraphic Modeling. Journal of Sedimentary Research, 75, 166-176.

Buckley, S.J., Howell, J.A., Enge, H.D., and Kurz, T.H. (2008). Terrestrial laser scanning in geology:Data acquisition, processing and accuracy considerations: Journal of the Geological Society, 165, 625–638.

Burnham, B., Hodgetts, D. (2018). Quantifying spatial and architectural relationships from fluvial outcrops. Geosphere, 15.

Carrillo, J., Forasiepi, A., Jaramillo, C., Sánchez-Villagra, M. (2014). Neotropical mammal diversity and the Great American Biotic Interchange: spatial and temporal variation in South America's fossil record. Frontiers in genetics. 5. 451. 10.3389/fgene.2014.00451.

Charlton, M., Coveney, S., Mccarthy, T. (2009). Laser Scanning for the Environmental Sciences: Issues in Laser Scanning.

Collinson, J. & Thompson., D. (1984). Sedimentary Structures. Second edition. George Allen & Unwin Ltd.

Fields, R. (1959). Geology of the La Venta badlands, Colombia, South America. University of California, Berkeley, 32, 405-444.

Flynn, J., Guerrero, J., Swisher, C. (1997). Geochronology of the Honda Group. In book: Vertebrate Paleontology in the Neotropics. The Miocene Fauna of La Venta, Colombia. Smithsonian Institution Press.

Folk, R. L. (1959). Practical petrographic classification of limestones. American Association of Petroleum Geologist - Bulletin, 43.

Guerrero, J. (1993). Magnetostratigraphic of the upper part of the Honda Group and Neiva formation. Miocene uplift of the Colombian Andes. Department of Geology, Duke University.

Hayashida, A. (1984). Paleomagnetic Study of the Miocene Continental Deposits in La Venta Badlands, Colombia. Department of Earth Sciences, Doshisha University.

Hodgetts, D. (2009). LiDAR in the Environmental Sciences: Geological Applications. 10.1002/9781444311952.ch11.

Miall, A.D. (1985). Architectural-element analysis: A new method of facies analysis applied to fluvial deposits. Earth-Science Reviews. 22. 261-308. 10.1016/0012-8252(85)90001-7.

Miall, A. D. 2006. The Geology of Fluvial Deposits. Sedimentary Facies, Basin Analysis, and Petroleum Geology. 4th edition. Springer.

Munsell (2009). Geological Rock-Color Chart. Geological Society of America.

Nesbit, P., Durkin, P., Hugenholtz, C., Hubbard, S., Kucharczyk, M. (2018). 3-D stratigraphic mapping using a digital outcrop model derived from UAV images and structure-from-motion photogrammetry. Geosphere. 14. 2469-2486.

Nichols, G. (2009). Sedimentology and stratigraphy. Oxford: Blackwell Science.

Ortiz, J., Moreno, C., Cárdenas, A., Jaramillo, C. (2015). SDAR 1.0 a new quantitative toolkit for analyze stratigraphic data. Geophys. Res.

Paola, C., Wiele, S., Reinhart, M. (1989). Upper-regime parallel lamination as the result of turbulent sediment transport and low-amplitude bed forms. Sedimentology, 36(1), 47–59.

Villarroel, C., Setoguchi, T., Bireva, J., Macia, C. 1996. Geology of the La Tatacoa "Desert" (Huila, Colombia): Precisions on the stratigraphy of the Honda group, the evolution of the "Pata high" and the presence of the La Venta fauna. Memoirs of the Faculty of science, Kyoto University. Series of geology and mineralogy. 58, 41-66.

Wellman, S. (1970). Stratigraphy and petrology of the Nonmarine Honda Group (Miocene), Upper Magdalena Valley, Colombia. Geological Society of America Bulletin, 81.

Wentworth, C. K. (1922). A scale of grade and class terms for clastic sediments. The Journal of Geology, 30(5), 377-392.

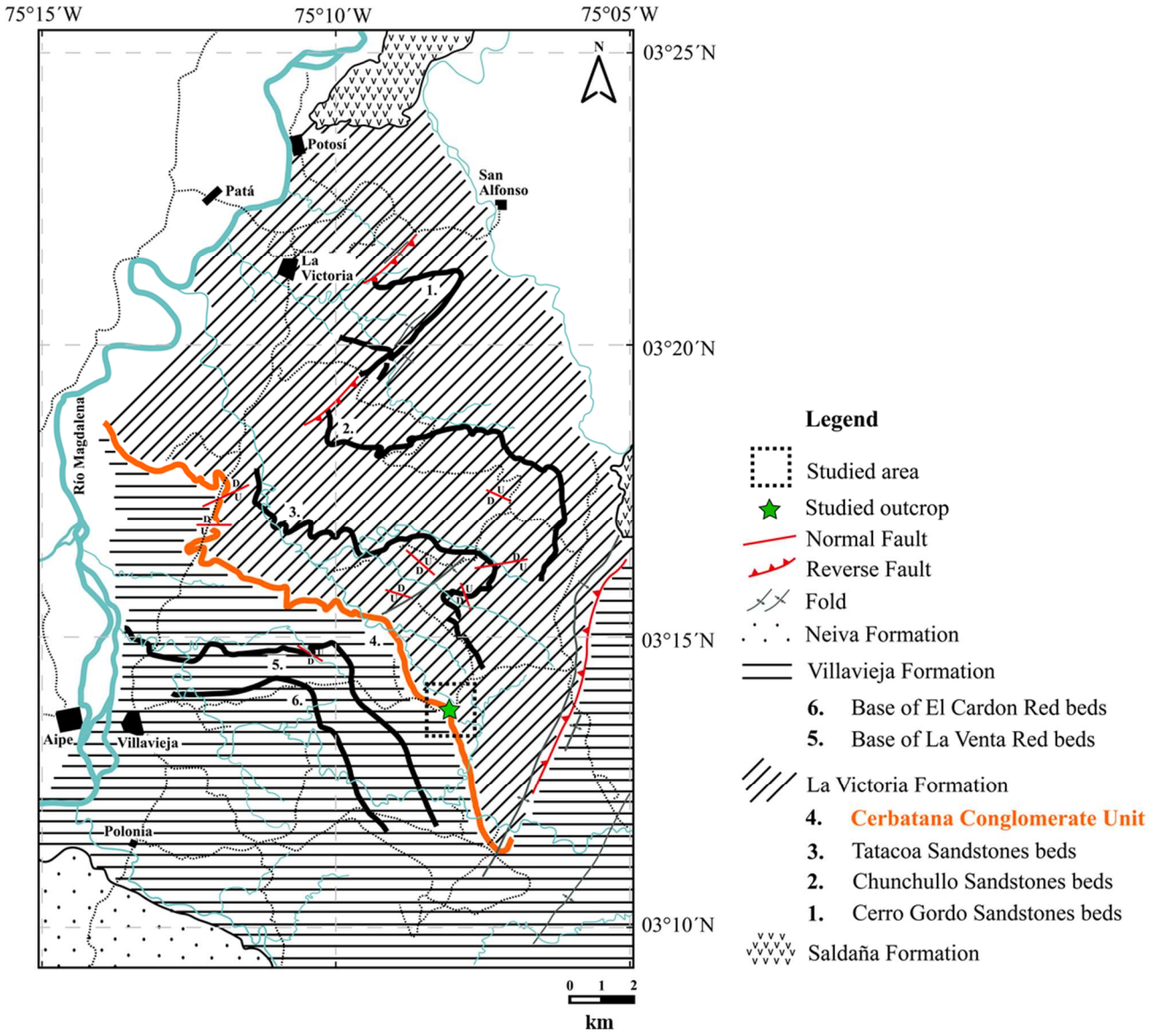

Figure 1. Geological map of La Venta site. The star indicates the location of the studied outcrop. Modified from Guerrero (1993).

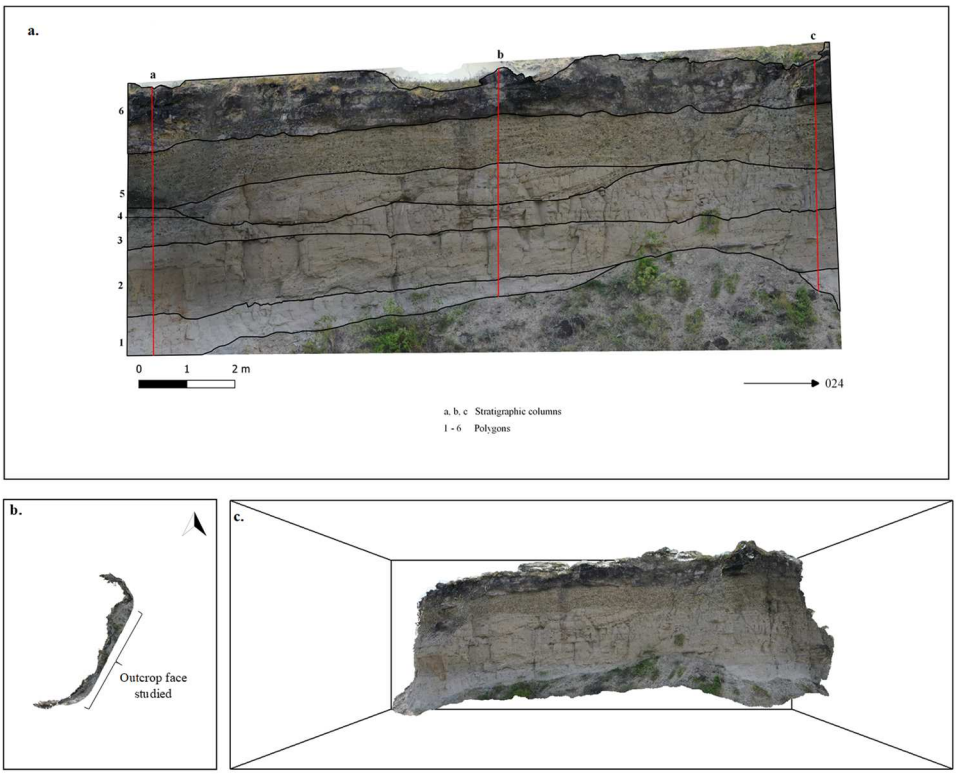

Figure 2. Digital models of the studied outcrop. (a) Orthomosaic showing the polygons defined with the outcrop mapping and field logs (i.e. stratigraphic columns). (b) Top view. (c) 3D Model.

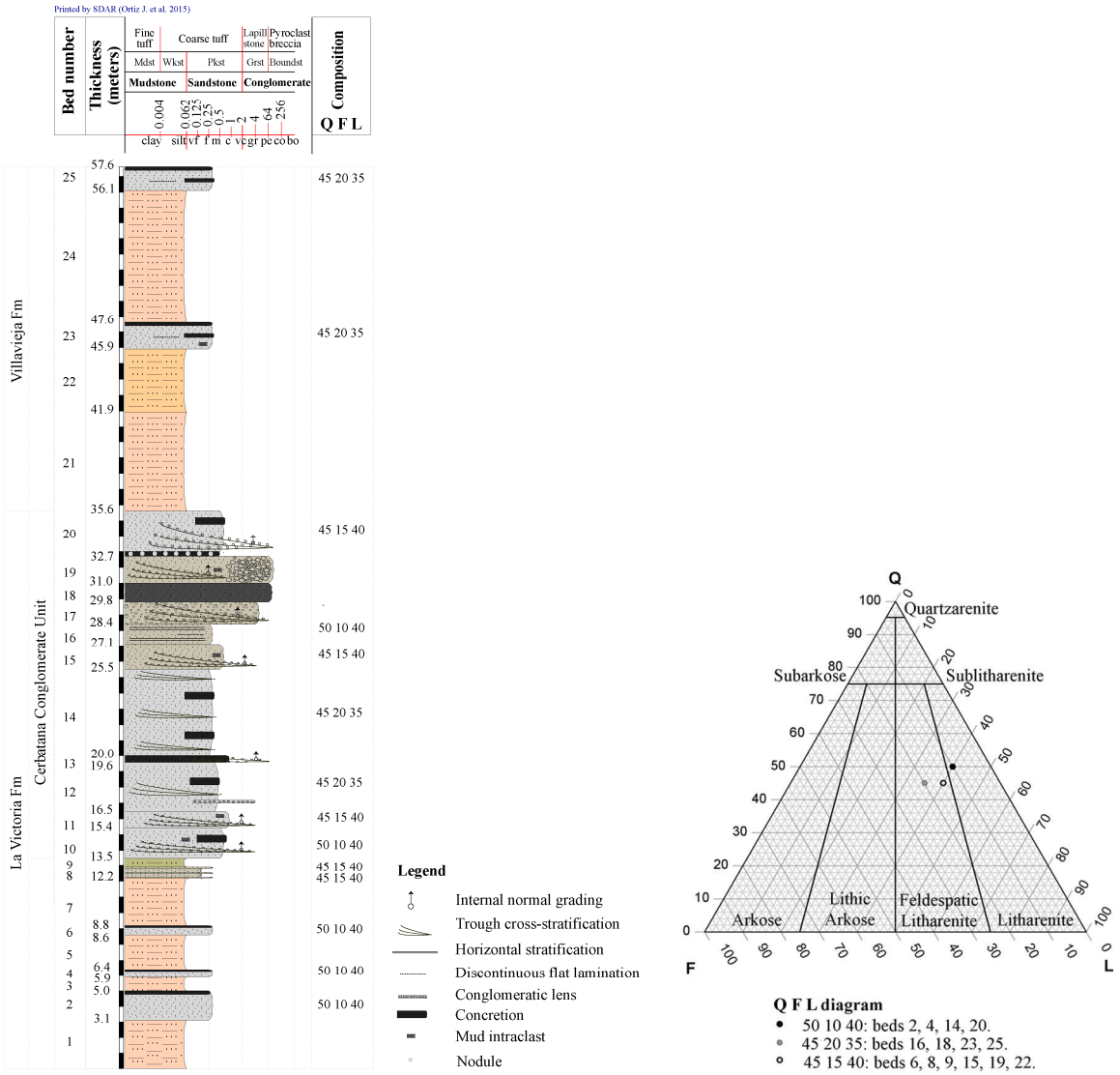

Figure 3. Left: stratigraphic column of the Honda Group in the southeast of the La Venta site, 57.6 meters of thickness. Right: QFL diagram (Folk, 1980).

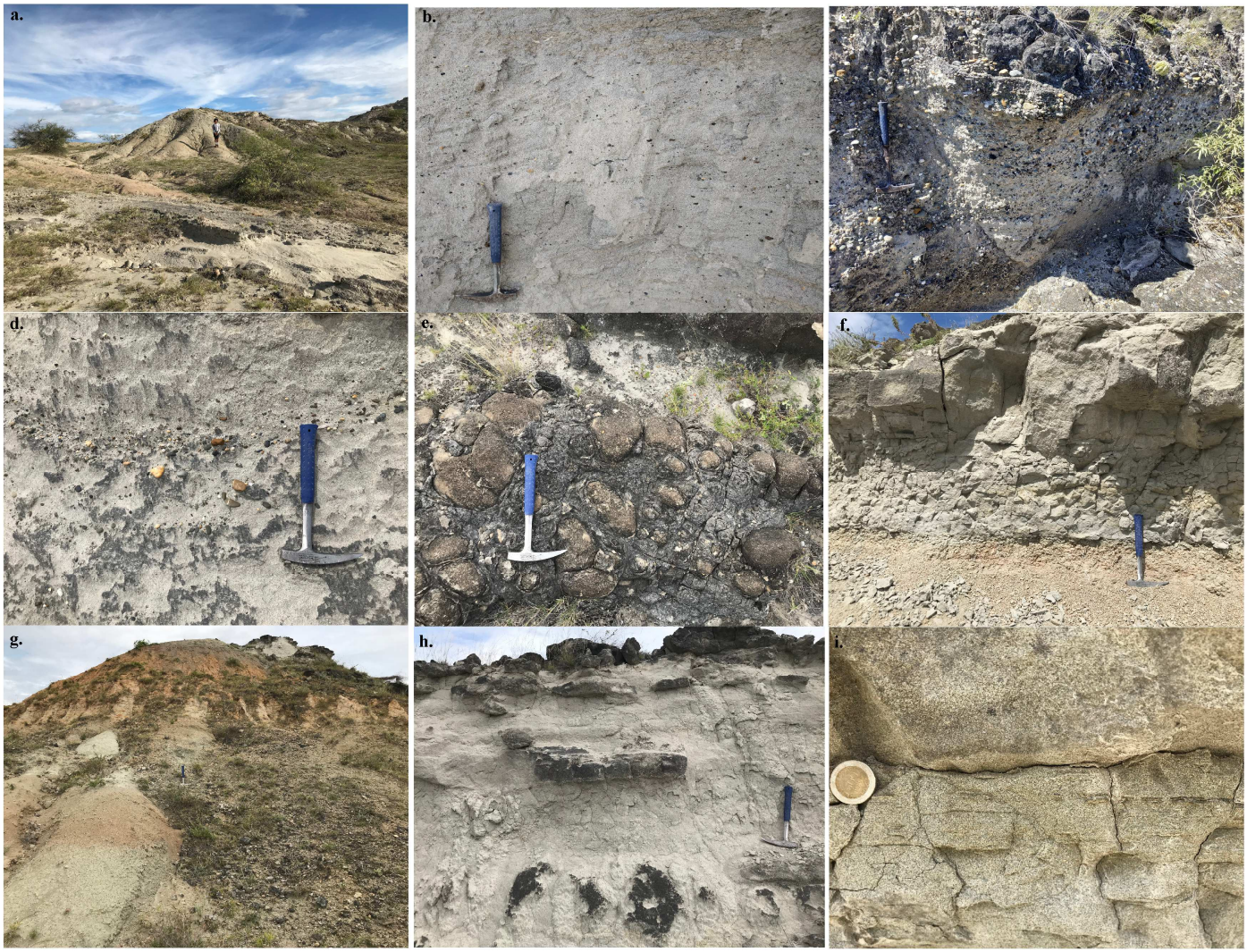

Figure 4. Photographs of the described Honda Group beds. (a) Siltstones with light red colors associated with paleosols – La Victoria Formation. (b) Mud intraclasts following the cross-stratification, bed 10. (c) Pebble-conglomeratic sandstones with trough cross-stratification, bed 19. (d) Medium trough cross-stratified sandstone with ordered imbricated fabric, bed 20. (e) Calcareous nodules and concretions with spheroidal weathering, base of bed 20. (f) Alternations of siltstones with massive fine-grained feldespathic litharenites, beds 21–25. (g) Siltstones with light red and reddish orange colors associated with paleosols, beds 21, 22 and 24. (h) Calcareous concretions at the top and within the beds, beds 23 and 25. (i) Discontinues flat laminations of heavy minerals, beds 23 and 25.

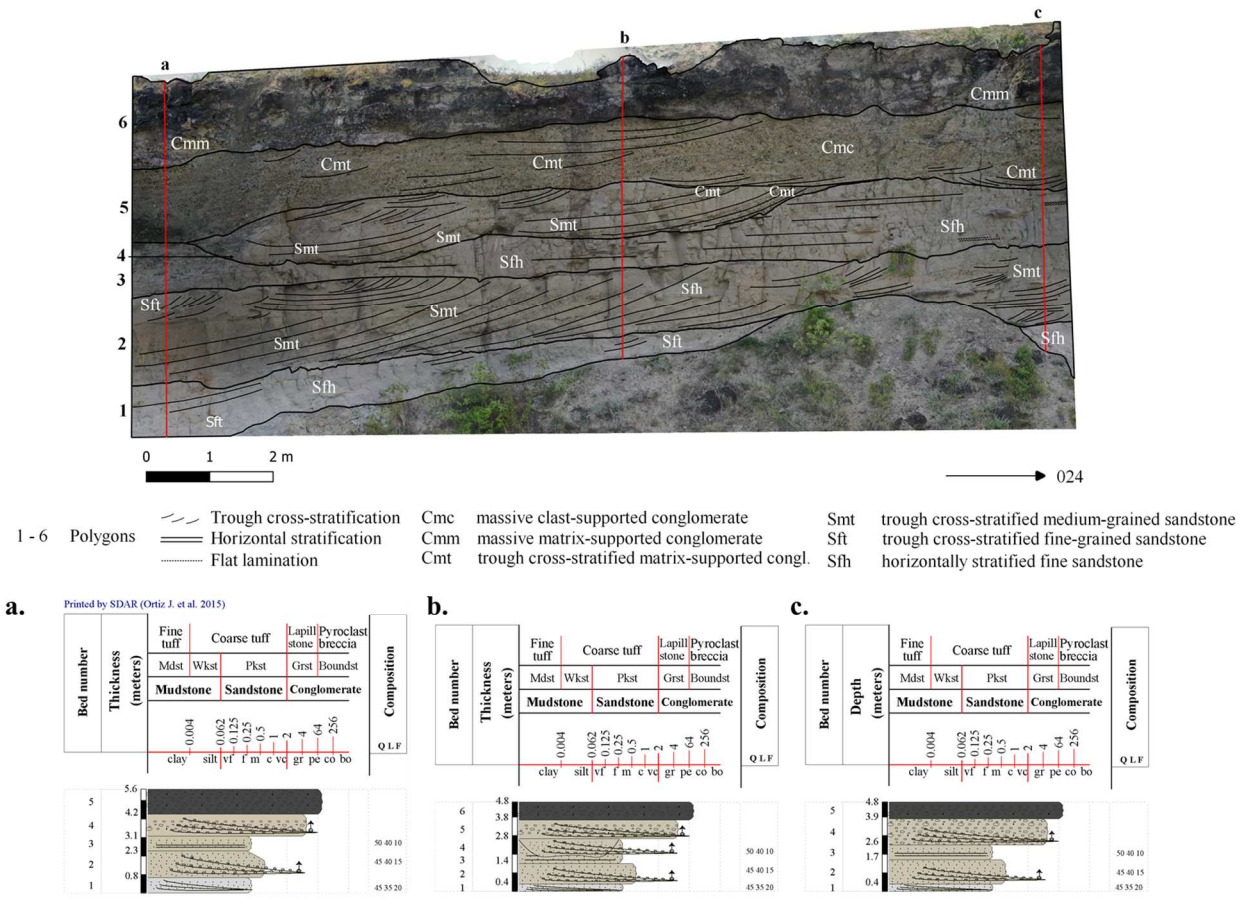

Figure 5. Facies defined in the studied outcrop from field log and orthomosaic analysis. 3 stratigraphic sections measured in both right and left corners and in the center (a, b and c).

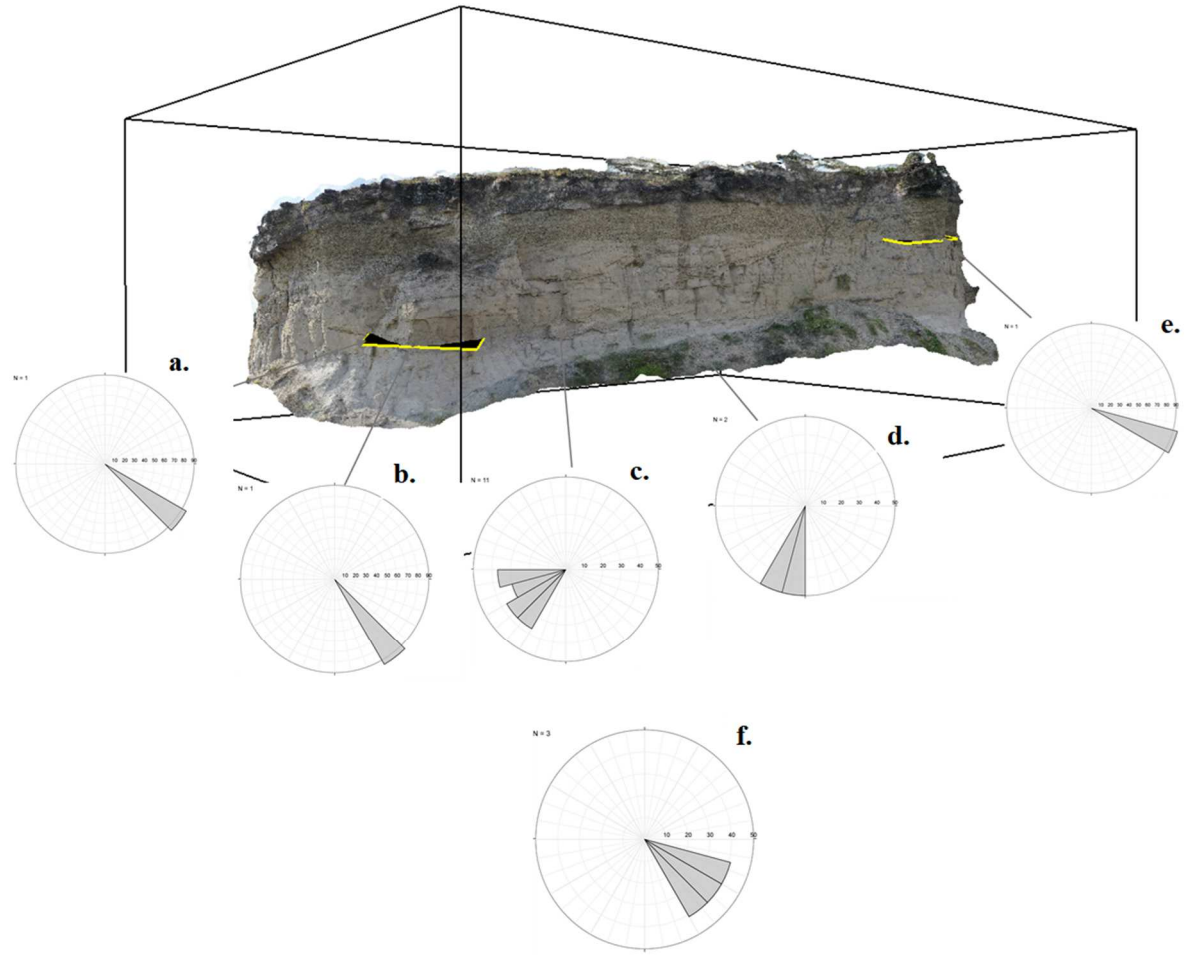

Figure 6. Paleocurrents analysis. (a) One plane measured in the 3D model obtaining the direction of the axis of trough cross-stratification in the polygon 2: 133°. (b) Field measurement of the axis direction in polygon 2: 149°. (c) Field measurement of eleven sets with one vertical face exposed of trough cross-stratification in the polygon 2 showing a tendency towards SW. (d) Field measurement of two sets with one vertical face exposed of trough cross-stratification in polygon 1 showing a tendency towards SW. (e) One plane measured in the 3D model obtaining the direction of the axis of trough cross-stratification in the polygon 5: 117°. (f) Data integration of the direction of axes measured in the field and from the 3D model showing a tendency towards the SE.

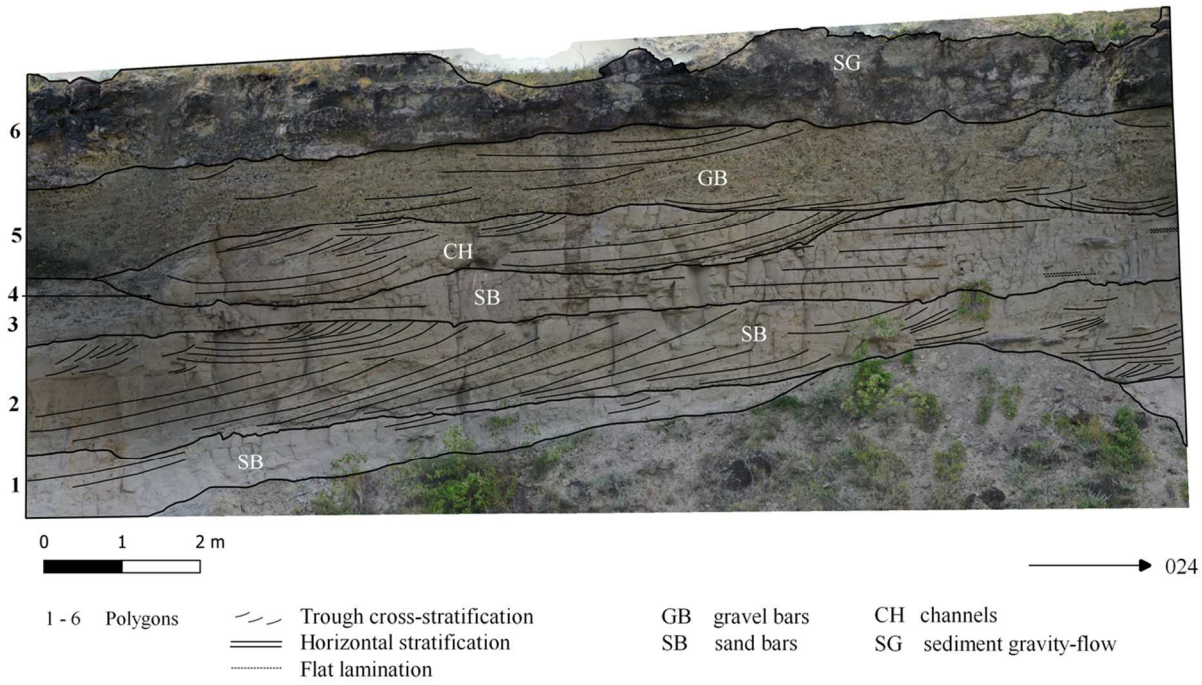

Figure 7. Stratigraphic architectural elements defined in the studied outcrop.

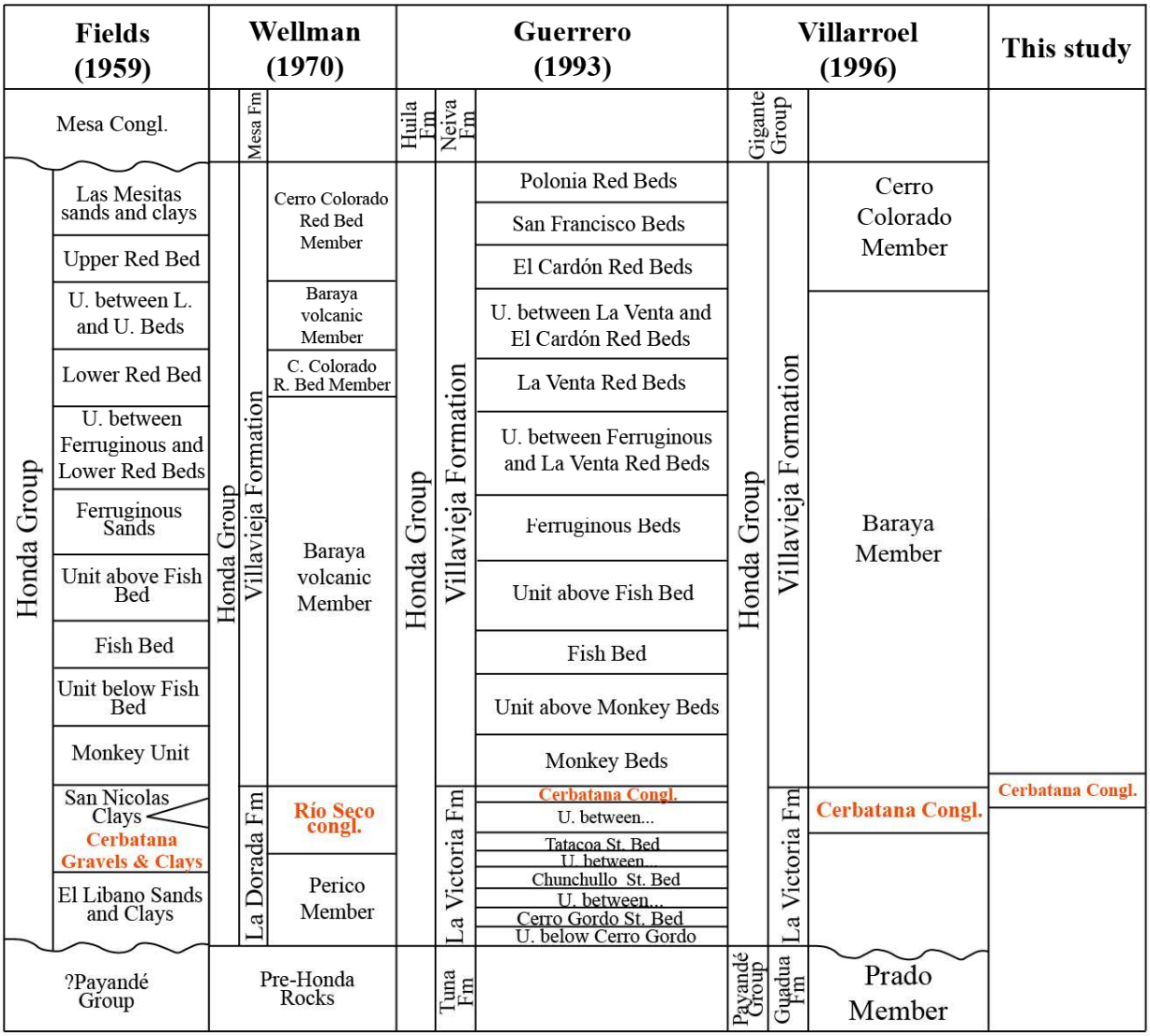

Figure 8. Correlation chart. Modified from Villarroel (1996).

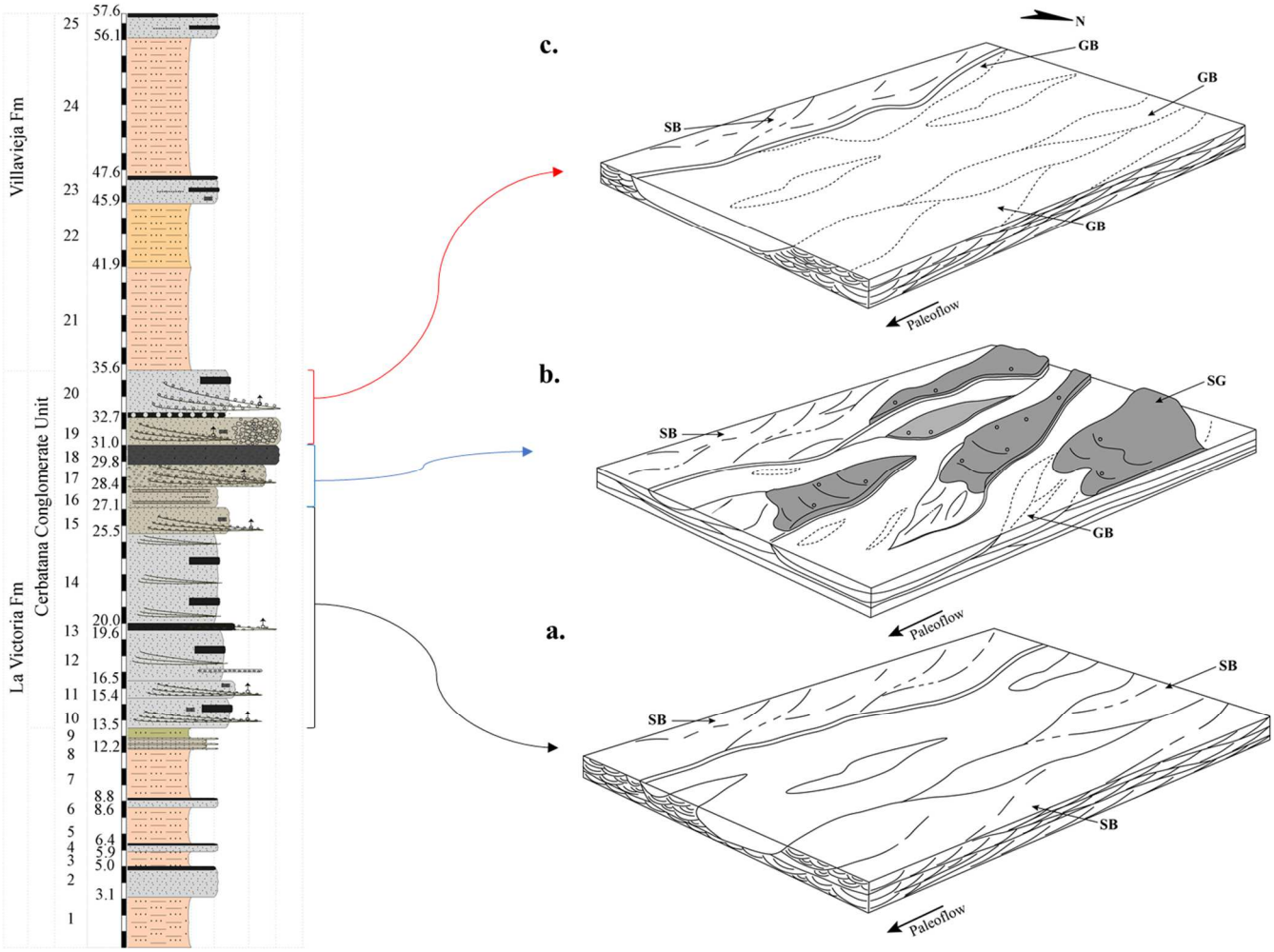

Figure 9. Depositional environment of the CCU. (a) sand-dominated braided river sequence, (b) and (c) gravel-dominated sequence. Modified from Miall (1985) and Nichols (2009).

Table 1. Field data and digital datasets integration.

	1	2	3	4	5	6
Measured thickness (m)	0.9	1.6	1.3	0.9	1.4	1.3
Width (m)	14.8	14.8	11 m	14.8	14.8	14.8
Lower contact change	-	sharp	sharp	sharp	sharp	sharp
Lower contact geometry	-	irregular	planar	concave	irregular	irregular
Original bed geometry	-	tabular	tabular	lenticular	tabular	tabular
Dominant Sedimentary Structure	trough cross stratification	trough cross stratification	horizontal stratification	trough cross stratification	trough cross stratification	massive
Strata position	mixed	mixed	-	mixed	mixed	-
Secondary sed. Structure	horizontal stratification	-	flat lamination	-	-	-
Strata position	mixed	-	to the right	-	-	-
Primary lithology	sandstone	sandstone	sandstone	sandstone	conglomerate	conglomerate
Grain size	fine	medium (with pebble content – 15%)	fine	medium	pebble	pebble
Matrix	very fine sand	fine sand	very fine sand	fine sand	medium to coarse sand	fine to medium sand
% matrix	< 5	< 5	< 5	< 5	25	50
Cement	siliceous	siliceous	siliceous	siliceous	siliceous	calcareous (secondary)
Roundness	rounded to sub rounded	rounded to sub rounded	rounded to sub rounded	rounded to sub rounded	rounded to sub rounded (pebbles)	rounded to sub rounded (pebbles)
Maximum grain size (cm)	-	4.2	-	-	5.7	6.0
Secondary lithology	sandstone	sandstone	-	conglomerate	conglomerate	-
Grain size	fine	fine	-	pebble	pebble	-
Matrix	very fine sand	very fine sand	-	fine sand	no identifiable	-
% matrix	< 5	< 5	-	20	no identifiable	-
Cement	siliceous	siliceous	-	siliceous	no identifiable	-
Roundness	rounded to sub rounded	rounded to sub rounded	-	rounded to sub rounded (pebbles)	no identifiable	-
Maximum grain size (cm)	-	-	-	4.5	5.6	-
Vertical gradation	-	internal normal gradation	-	internal normal gradation	-	-
Sorting (primary lithology)	well	moderately	well	well	poorly	very poorly
Fresh color (Munsell)	10Y 8/2 (pale greenish yellow)	5Y 8/4 (grayish yellow)	5Y 8/4 (grayish yellow)	5Y 8/4 (grayish yellow)	5Y 8/4 (grayish yellow)	5Y 8/4 (grayish yellow)
Sandstone composition (Q F L)	45 20 35	45 15 40	50 10 40	-	-	-
Classification Folk (1980)	feldspathic litharenite	feldspathic litharenite	litharenite	-	-	-
Dominant lithofacies	trough cross-stratified fine-grained sandstone	trough cross-stratified medium-grained sandstone (with pebble content)	horizontally stratified fine sandstone	trough cross-stratified medium-grained sandstone	trough cross-stratified matrix-supported conglomerate	massive matrix-supported conglomerate
% dominant lithofacies	50	95	100	60	90	100
Secondary lithofacies	horizontally stratified fine sandstone	trough cross-stratified fine-grained sandstone	-	trough cross-stratified matrix-supported conglomerate	massive clast-supported conglomerate	-
% secondary lithofacies	50	5	-	40	10	-

Table 2. Paleocurrents measurements from fieldwork and 3D model.

Polygon	# Set	Dip	Dip direction	Type of data	From
1	1	14	209	one vertical face exposed	field data
	2	20	190	one vertical face exposed	field data
2	1	20	250	one vertical face exposed	field data
	2	16	263	one vertical face exposed	field data
	3	14	213	one vertical face exposed	field data
	4	12	235	one vertical face exposed	field data
	5	12	221	one vertical face exposed	field data
	6	18	239	one vertical face exposed	field data
	7	20	268	one vertical face exposed	field data
	8	16	260	one vertical face exposed	field data
	9	16	250	one vertical face exposed	field data
	10	18	237	one vertical face exposed	field data
	11	13	220	one vertical face exposed	field data
	12	19	149	axis	field data
	12	22	133	axis	3D model
5	1	12	117	axis	3D model

Table 3. Facies defined in the studied outcrop.

id	Lithofacies	Description	Interpretation
Cmm	Massive matrix supported conglomerate.	Massive, very poorly sorted, pebble conglomerate with sub-rounded to rounded clasts. Fine to medium sandy matrix. Maximum pebble size: 6 cm. Secondary calcareous cement.	Poor sorting and absence of sedimentary structures may be associated to debris flows deposition by gravity flow transport (Collinson and Thompson, 1982; Miall, 1985).
Cmt	Trough cross-stratified matrix supported conglomerate.	Poorly sorted, granule- to- pebble conglomerate with sub-rounded to rounded clasts. Medium to coarse-grained matrix in a proportion of 25%. Maximum pebble size: 5.7 cm. Trough cross stratification with ordered imbricated fabric.	Trough cross stratification records the migration of channel bed forms by traction-dominated bedload (Collinson and Thompson, 1982; Miall, 1985).
Cmc	Massive clast-supported conglomerate.	Massive, clast supported pebble conglomerate. This lithofacies is mixed with Cmt. Maximum pebble size: 5.6 cm. Imbricated grains in some cases.	Pebbles indicate high energy flow condition by a traction-dominated bedload (Collinson and Thompson, 1982; Miall, 1985).
Sfh	Planar horizontally stratified fine sandstone.	Well-sorted fine-grained sandstone with sub-rounded to rounded grains, and discontinuous flat lamination of heavy minerals.	Turbulent sediment transport reflecting migration of low-amplitude bed forms under an upper flow regime (Collinson and Thompson; Paola et al., 1989).
Sft	Trough cross-stratified fine-grained sandstone.	Well-sorted fine-grained sandstone with sub-rounded to rounded grains. Trough cross stratification with ordered imbricated fabric. Mixed with Sfh facies.	Traction-dominated bedload, trough cross stratification records the migration of channel bed forms (Collinson and Thompson, 1982; Miall, 1985).
Smt	Trough cross-stratified medium grained sandstone.	Moderately sorted medium grained sandstone with sub-rounded to rounded grains. This sandstone has a granully to pebbly admixture. Maximum pebble size: 4.2 cm. Trough-cross stratification with ordered imbricated fabric.	Trough cross stratification records the migration of channel bed forms by traction-dominated bedload, and pebbles indicate high energy flow conditions (Collinson and Thompson, 1982; Miall, 1985).